

Quenched Fe moment in the collapsed tetragonal phase of $\text{Ca}_{1-x}\text{Pr}_x\text{Fe}_2\text{As}_2^*$

Ma Long(马龙)^{a)}, Ji Gao-Feng(吉高峰)^{a)}, Dai Jia(代佳)^{a)}, Saha S R^{b)}, Drye T^{b)}, Paglione J^{b)},
and Yu Wei-Qiang(于伟强)^{a)†}

^{a)}Department of Physics, Renmin University of China, Beijing 100872, China

^{b)}Center for Nanophysics and Advanced Materials, Department of Physics, University of Maryland, College Park, MD 20742, USA

(Received 27 February 2013; revised manuscript received 12 March 2013)

We report ^{75}As NMR studies on single crystals of rare-earth doped iron pnictide superconductor $\text{Ca}_{1-x}\text{Pr}_x\text{Fe}_2\text{As}_2$. In both cases of $x = 0.075, 0.15$, a large increase of ν_Q upon cooling is consistent with the tetragonal-collapsed tetragonal structure transition. A sharp drop of the Knight shift is also seen just below the structure transition, which suggests the quenching of Fe local magnetism, and therefore offers important understanding of the collapsed tetragonal phase. At even low temperatures, the $1/^{75}T_1$ is enhanced and forms a peak at $T \approx 25$ K, which may be caused by the magnetic ordering of the Pr^{3+} moments or spin dynamics of mobile domain walls.

Keywords: quenched Fe moment, collapsed tetragonal phase, iron pnictides, nuclear magnetic resonance

PACS: 74.70.Xa, 74.25.nj, 76.60.-k

DOI: 10.1088/1674-1056/22/5/057401

1. Introduction

The interplay of structure, magnetism, and superconductivity is one essential ingredient in understanding high-temperature superconductivity in the iron-based superconductors. At low temperatures, superconductivity usually occurs in the tetragonal (\mathcal{T}) phase upon carrier doping or under pressure,^[1–5] which suppresses the antiferromagnetic, orthorhombic (\mathcal{O}) phase seen in the parent compounds. Recently, a high-temperature tetragonal to a low-temperature collapsed tetragonal ($c\mathcal{T}$) phase has also been reported by pressure or doping in many iron pnictides, such as CaFe_2As_2 ($P \geq 0.3$ GPa),^[6–8] $\text{Ca}_{1-x}\text{R}_x\text{Fe}_2\text{As}_2$ ($P = 0$, $R = \text{Pr, Nd}$),^[9,10] BaFe_2As_2 ($P \geq 27$ GPa),^[11] EuFe_2As_2 ($P \geq 8$ GPa),^[12] and $\text{CaFe}_2(\text{As}_{1-x}\text{P}_x)_2$ ($P = 0$).^[13] For the first two compounds, superconductivity is also found, accompanying the emergence of the $c\mathcal{T}$ phase at low temperatures, although with a small volume ratio.^[6,8–10] It is now known that CaFe_2As_2 has a T_C of about 12 K in liquid pressure cell,^[7,8] but loses superconductivity in the pure $c\mathcal{T}$ phase under hydrostatic conditions.^[14] Local probe studies show that superconductivity occurs in the residual \mathcal{T} phase,^[15,16] which may be located at the interface of the \mathcal{O} phase and the $c\mathcal{T}$ phase coexisting under inhomogeneous pressure.^[14]

In several rare-earth doped $\text{Ca}_{1-x}\text{R}_x\text{Fe}_2\text{As}_2$, both the structure collapse and superconducting transitions with T_C almost equal to 10 K and 45–47 K have been reported.^[9,10] The low T_C phase is probably an analogy to CaFe_2As_2 under

pressure.^[10] Although rare-earth substitution may induce electron doping, the high- T_C phase remains unclear since its T_C is the highest among the pnictides with the ThCr_2Si_2 (122) structure, including the electron-doped $\text{Ca}(\text{Fe}_{1-x}\text{Co}_x)_2\text{As}_2$.^[17] Experimentally, the structure collapse is characterized by a large shrinkage of the c -axis lattice parameter (or the c/a ratio) induced by external or chemical pressure.^[7,9,18] For CaFe_2As_2 , high-pressure inelastic neutron scattering studies indicate that the dynamic magnetic correlations are suppressed at the antiferromagnetic wave vector ($\pi/a, \pi/a$) in the $c\mathcal{T}$ phase,^[19] whereas correlations at other momentum have not been investigated yet. Theoretical studies suggest that the short As–As interlayer distance could lead to suppressed Fe moments either in the high-temperature \mathcal{T} phase^[20] or in the low-temperature $c\mathcal{T}$ phase.^[13,21,22] All these different scenarios should be further studied in order to reveal the nature of the $c\mathcal{T}$ phase and also the high- T_C phase.

In this report, we present ^{75}As ($S = 3/2$) NMR studies on $\text{Ca}_{1-x}\text{Pr}_x\text{Fe}_2\text{As}_2$ ($x = 0.075, 0.15$) superconducting single crystals. The structure collapse is shown by the frequency shift of the ^{75}As satellites. The magnetic properties of the $c\mathcal{T}$ phase are studied by the Knight shift ^{75}K and the spin-lattice relaxation rate $1/^{75}T_1$. Our ^{75}K drops sharply with temperature below the structure transition, which indicates that the Fe paramagnetic moments are suppressed in the $c\mathcal{T}$ phase. The spin-lattice relaxation rate $1/^{75}T_1$, on the other hand, is enhanced below T_S and forms a prominent peak at $T^* \sim 25$ K,

*Project supported by the National Natural Science Foundation of China (Grant Nos. 11074304 and 11222433) and the National Basic Research Program of China (Grant Nos. 2010CB923004 and 2011CBA00112). Work at the University of Maryland supported by AFOSR-Multidisciplinary University, Research Initiative (Grant No. FA9550-09-1-0603).

†Corresponding author. E-mail: wqyu_phy@ruc.edu.cn

which is likely to be caused by the magnetic ordering of Pr^{3+} or the dynamics of mobile domain walls. Our data reveals the correlation effect between the magnetic properties and the lattice structure, which should be important for understanding the nature of the $c\mathcal{T}$ phase, and may also be helpful for understanding the mechanism of superconductivity.

2. Experimental details

The $\text{Ca}_{1-x}\text{Pr}_x\text{Fe}_2\text{As}_2$ single crystals were synthesized by the FeAs self-flux method with details reported previously.^[23] For our NMR experiments, large crystals with areas of $5 \times 5 \text{ mm}^2$ and thickness of 0.5 mm (c -axis) were chosen. We studied two compositions, $x = 0.075$ and 0.15 (determined by WDS), which were characterized by the SQUID susceptibility measurements (shown later). The NMR experiments are carried out using the standard coherent pulse method. The sample is placed on a rotator to allow us to change field orientations, and the frequency-swept NMR spectra are obtained by integrating the intensity of the Fourier transform of the spin echo signal. The spin-lattice relaxation rate $1/T_1$ is obtained by the inversion-recovery method. Most data are collected during warming up for consistency, except the hysteresis loop.

3. Superconductivity, chemical pressure effect, and structure collapse

The susceptibility data of both dopings are shown in Fig. 1, where the superconducting transition and the structure transition are evident. For $x = 0.075$, superconductivity occurs at $T_c \sim 25 \text{ K}$ with a 1 mT in-plane field (Fig. 1(a)), and superconducting volume ratio is estimated to be $\sim 0.2\%$. The $x = 0.15$ doping has a higher T_c ($\sim 35 \text{ K}$) and a larger superconducting volume ($\sim 2\%$) as shown in Fig. 1(c). With a 0.1 T magnetic field, the superconductivity of both crystals is suppressed, as shown in Figs. 1(b) and 1(d), which is consistent

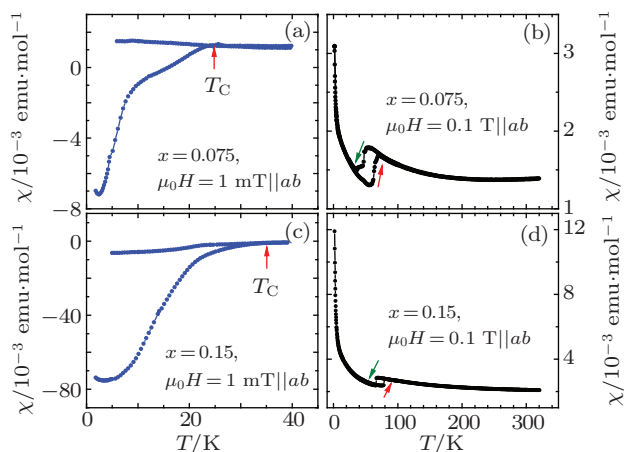


Fig. 1. (color online) dc susceptibility as a function of temperature for the $x = 0.075$ and $x = 0.15$ samples respectively. (a) and (c) show the susceptibility under a magnetic field of 1 mT, and (b) and (d) under a higher field of 0.1 T, with fields applied along the crystalline ab -plane.

with filamentary superconductivity reported previously.^[9,10] Furthermore, the susceptibility under 0.1 T field shows a clear hysteresis loop at higher temperatures, corresponding to a \mathcal{T} to $c\mathcal{T}$, first-order structural phase transition.^[9] The transition temperature T_S is about 64 K (warming) and 48 K (cooling) for the $x = 0.075$ doping, and 78 K (warming) and 66 K (cooling) for the $x = 0.15$ doping.

The ^{75}As NMR spectra at typical temperatures are shown in Figs. 2(a) and 2(b) for two crystals. We note here that superconductivity, as measured by diamagnetic screening, is already suppressed by the large NMR field. Figure 2(a) shows the ^{75}As NMR spectra for the $x = 0.075$ crystal, with a central transition ($f \approx 74.5 \text{ MHz}$) and a high-frequency satellite ($f \approx 83 \text{ MHz}$ at 80 K and $f \approx 90.7 \text{ MHz}$ at 1.5 K), with a 10 T field applied in the ab plane. Similar spectra for the $x = 0.15$ crystal are shown in Fig. 2(c) with an 11.5 T field applied along the c axis.

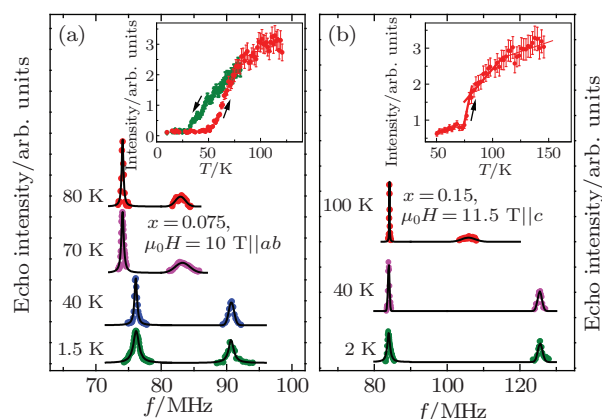


Fig. 2. (color online) The ^{75}As NMR spectra at typical temperatures for (a) the $x = 0.075$ crystal with a 10 T field applied in the crystalline ab -plane and (b) the $x = 0.15$ crystal with an 11.5 T field applied along the c -axis. Inset: the temperature dependence of the spectral weight fixed at the central transition of the \mathcal{T} phase, with arrows indicating the warming (cooling) direction.

The large frequency shift of the satellite upon cooling, as shown in Fig. 2, is an indication of the structure transition. Since ^{75}As has a local fourfold in-plane symmetry, the principal axis of the electric field gradient is along the c axis. The nuclear quadrupole resonance frequencies (ν_q) can be estimated by the angular dependence of the satellite, $f = \nu_L(1 + K) \pm \nu_q(3 \cos^2 \theta - 1)/2$, where ν_L and K represent the Larmor frequency and the Knight shift, and θ represents the angle from the field orientation to the crystalline c axis. Since K is small (shown later), the shift of the high-frequency satellites is primarily caused by the increase of ν_q upon structure collapse, because of the reduced c lattice parameter.^[9] The ν_q increase from 20.4 MHz to 35.8 MHz by structure collapse for $x = 0.075$, and 21.6 MHz to 41.5 MHz for $x = 0.15$. Furthermore, the frequency of the central transition also changes by structure collapse (Figs. 2(a) and 2(b)), due to a second-

order quadrupole correction

$$f = (1 + K)v_L + \frac{-3v_Q^2}{16v_L}(1 - \cos^2\theta)(9\cos^2\theta - 1).$$

The inset in Figs. 2(a) and 2(b) shows the temperature dependence of the spectral weight at the central transition of the \mathcal{T} phase. The drop and the thermal hysteresis loop of the spectral weight are consistent with the structure transition revealed by the susceptibility data.

We further look at the high-temperature \mathcal{T} phase at different dopings. In the \mathcal{T} phase, the v_q is estimated to be ~ 20.4 MHz for $x = 0.075$ and ~ 21.6 MHz for $x = 0.15$. For comparison, the v_q of CaFe_2As_2 increases with pressure from 11.8 MHz at $P = 0$ to 25 MHz at $P = 1.08$ GPa.^[16] The large increase of v_q with Pr^{3+} doping in $\text{Ca}_{1-x}\text{Pr}_x\text{Fe}_2\text{As}_2$ is consistent with a chemical pressure effect to induce the structure collapse.

4. Quenched Fe moment in the $c\mathcal{T}$ phase

With field applied along the c axis ($\theta = 0$), the quadrupole correction to the central transition is zero. Then the Knight shift can be calculated from the central frequencies by ${}^{75}K(T) = (f - {}^{75}\gamma B)/{}^{75}\gamma B$, where ${}^{75}\gamma = 7.292$ MHz/T is the gyromagnetic ratio of ${}^{75}\text{As}$, and f is the resonance frequency under field B . Figures 3(a) and 3(b) show the central transition for two dopings at typical temperatures with field applied along the c axis. With reduced temperature, the central frequency shifts to low frequency and the spectra become broadened significantly. The Knight shift and the NMR linewidth

are obtained from the Gaussian fit to the spectra, and depicted as a function of temperature in Figs. 3(c) and 3(d). The Knight shift of the undoped CaFe_2As_2 ^[24] is also plotted for comparison.

The Knight shift barely changes with temperature above T_S . Just below T_S , however, ${}^{75}K(T)$ drops sharply with temperature. The drop of ${}^{75}K(T)$ through the T_S is unlikely to be caused by a Pauli paramagnetic effect for the following reason. Transport measurements suggest that the carrier density on the Fermi surface increases through the structure collapse,^[9] which in principle should not lead to a large decrease of ${}^{75}K$ from Pauli paramagnetic contributions. Therefore, we think that the decrease of ${}^{75}K(T)$ originates from a reduced spin correlation effect. Since the NMR Knight shift K is proportional to $\chi(q = 0)$, where $\chi(q = 0)$ is the electron susceptibility, the reduced $K(T)$ signifies a large suppression of local paramagnetic spin fluctuations of Fe upon structure collapse. In particular $K(T) \approx 0$ at $T = 2$ K, which suggest that the Fe moment is almost zero in the $c\mathcal{T}$ phase. Similar reduction of ${}^{75}K(T)$ is also obtained for $x = 0.15$ below T_S , as shown in Fig. 3(c).

Our data clarifies that the paramagnetism is quenched in the $c\mathcal{T}$ phase^[21] and not in the \mathcal{T} phase^[20] in our case, and expands the inelastic neutron scattering study beyond the AFM wave vector.^[19] To our knowledge, this is the first experimental evidence for the quenched Fe moment in the $c\mathcal{T}$ phase, which suggests that the Fe moment is very sensitive to the pnictogen height, or the Fe–As–Fe bond angle, in the iron-based materials, and should be important for understanding the nature of the $c\mathcal{T}$ phase.

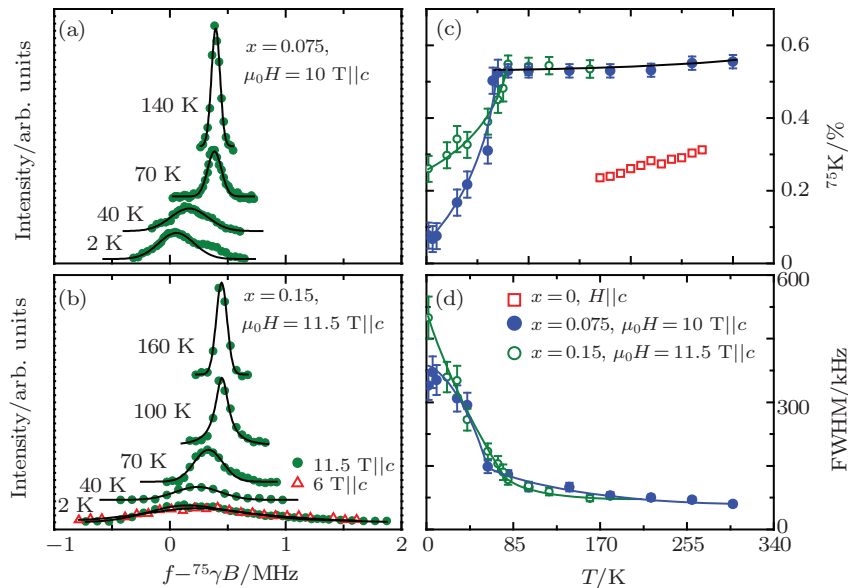


Fig. 3. (color online) (a) The ${}^{75}\text{As}$ spectra of the central transition of the $x = 0.075$ sample at typical temperatures with 10 T field along the c axis. (b) The ${}^{75}\text{As}$ spectra of the central transition of the $x = 0.15$ sample at typical temperatures with 6 T and 11.5 T field along the c axis. (c) The ${}^{75}\text{As}$ Knight shifts of $\text{Ca}_{1-x}\text{Pr}_x\text{Fe}_2\text{As}_2$ ($x = 0, 0.075, 0.15$) as a function of temperature. The $x = 0$ data are adapted from Ref. [24]. (d) The FWHM of the ${}^{75}\text{As}$ central transition as a function of temperature for two dopings.

5. Slow spin dynamics observed in the low-temperature region

Below T_S , the ^{75}As NMR linewidth starts to increase significantly upon cooling as shown in Fig. 3(b) and 3(d). For $x = 0.15$, the line width increases from 100 kHz to 500 kHz when cooled to 2 K, although the spin-spin relaxation time is very long ($T_2 \approx 5$ ms). We further checked the field dependence of the ^{75}As spectra at $T = 2$ K, as shown in Fig. 3(b). The NMR linewidth is almost the same with two different fields 6.5 T and 11.5 T, which suggests that the broadening is not caused by a quadrupole effect ($\Delta f \propto 1/H$) or a Knight shift effect ($\Delta f \propto H$). In fact, our data is consistent with a magnetic ordering effect, which is static within the NMR time scale.

We further search for evidence of magnetic ordering from the spin-lattice relaxation rate $1/^{75}T_1$. In Fig. 4, the temperature dependence of the $1/^{75}T_1$ is shown for CaFe_2As_2 and our doped samples. At high temperatures, $1/^{75}T_1$ is proportional to temperature, as shown by the straight line. Below T_S , however, a large increase of $1/^{75}T_1$ is clearly seen for our doped samples, and $1/^{75}T_1$ forms a broad peak at $T^* \approx 25$ K. Below T^* , $1/^{75}T_1$ decreases again with cooling. In fact, the $1/T_1$ above T^* follows a Curie-Weiss behavior with $1/T_1 T = A/(T + \theta) + b$, as shown by the solid line in the main panel of Fig. 4. The Curie-Weiss form and the peak behaviors in $1/^{75}T_1 T$ are also consistent with a magnetic ordering of itinerant magnetic systems.^[25]

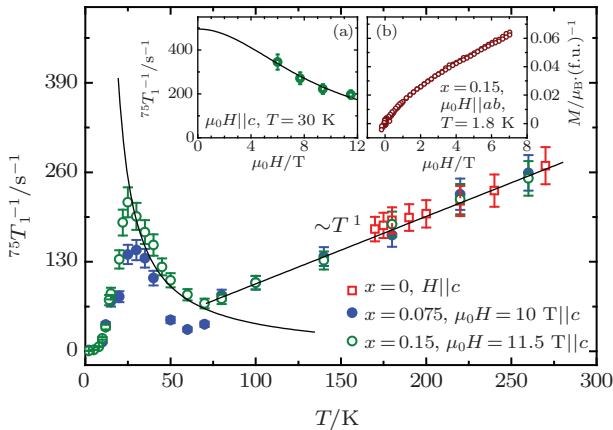


Fig. 4. (color online) The ^{75}As spin-lattice relaxation rate ($1/^{75}T_1$) of $\text{Ca}_{1-x}\text{Pr}_x\text{Fe}_2\text{As}_2$ as a function of temperature with $x = 0$ (adapted from Ref. [24]), 0.075, and 0.15. The curved solid line is a fit to the Curie-Weiss function (see text). Inset (a) The spin-lattice relaxation rates of the $x = 0.15$ sample as a function of field at $T = 30$ K. The black solid line is a guide for the eye. Inset (b) The dc magnetization of the $x=0.15$ sample as a function of field applied along the ab plane.

The sharp drop of $^{75}K(T)$ at T_S and the peak of $1/^{75}T_1$ far below T_S suggests that these two have very different magnetic origins. The low-temperature magnetic ordering is likely caused by Pr^{3+} moments, and not from Fe moments for three reasons. First, in PrFeAsO ^[26,27] and $\text{PrFeAsO}_{1-x}\text{F}_x$,^[28] Pr^{3+}

magnetic ordering has been reported with a peak behavior in $1/^{75}T_1$ at $T^* \approx 10$ K. The magnetic interactions of Pr^{3+} are likely caused by the Ruderman-Kittel-Kasuya-Yoshida (RKKY) interactions. The higher T^* in $\text{Ca}_{1-x}\text{Pr}_x\text{Fe}_2\text{As}_2$ is consistent with stronger RKKY interactions from larger carrier densities and/or smaller c -axis lattice parameters in the $c\mathcal{T}$ phase. Second, in the inset of Fig. 4, the $1/T_1$ under different fields are shown at $T = 30$ K for the $x = 0.15$ doping, where the $1/^{75}T_1$ decreases by 1.5 times with field increases from 6 T to 11.5 T. Such field behavior is typical for weakly magnetic metals,^[29] where the magnetic moment is small, or the magnetism is weakly coupled to the itinerant electrons. Finally, the low-temperature dc susceptibility, as shown Figs. 1(b) and 1(d), has a significant low-temperature upturn, which is also in support of magnetic ordering of rare earths. In contrast, $\text{Ca}_{0.85}\text{La}_{0.15}\text{Fe}_2\text{As}_2$ does not have a large upturn^[9] because La^{3+} is non-magnetic.

However, we cannot overrule that the mobile domain walls may dominantly contribute to such a low temperature critical slowing down behavior in $1/T_1$. In CaFe_2As_2 parent compound, slow fluctuation of hyperfine field at $T \sim 10$ K is observed to be caused by mobile antiphase domain walls and shows strong field dependence.^[30] At these antiphase domain boundaries, filamentary superconductivity is found to nucleate. Such slow spin dynamics evidenced from $1/T_1$ measurements in our Pr doped CaFe_2As_2 samples, may also be attributed to the dynamics of mobile domain walls below the structure transition and suggest that the filamentary superconductivity with such a high T_C may also be located on the domain boundaries.

6. Conclusions

To summarize, we have carried out the ^{75}As NMR to study the collapsed tetragonal phase on the rare-earth doped superconductors $\text{Ca}_{1-x}\text{Pr}_x\text{Fe}_2\text{As}_2$ ($x = 0.075$ and 0.15) for the first time. The chemical pressure effect by doping and the structure collapse are identified from the change of the v_q . The Knight shift, the linewidth, and the spin-lattice relaxation rate suggest that the Fe moment is strongly suppressed through the structure collapse. In the collapsed tetragonal phase, slow fluctuation of the hyperfine field is evidenced from $1/T_1$ measurements, which may be caused by a magnetic ordering of Pr^{3+} moment or spin dynamics of mobile domain walls. The suppression of Fe moment below T_S suggests a strong coupling between the lattice structure and the magnetism in the iron pnictides.

References

- [1] Kamihara Y, Watanabe T, Hirano M and Hosono H 2008 *J. Am. Chem. Soc.* **130** 3296
- [2] Chen X H, Wu T, Wu G, Liu R H, Chen H and Fang D F 2008 *Nature* **453** 761

- [3] Ren Z A, Lu W, Yang J, Yi W, Shen X L, Li Z C, Che G C, Dong X L, Sun L L, Zhou F and Zhao Z X 2008 *Chin. Phys. Lett.* **25** 2215
- [4] Chen G F, Li Z, Wu D, Li G, Hu W Z, Dong J, Zheng P, Luo J L and Wang N L 2008 *Phys. Rev. Lett.* **100** 247002
- [5] Rotter M, Tegel M and Johrendt D 2008 *Phys. Rev. Lett.* **101** 107006
- [6] Torikachvili M S, Bud'ko S L, Ni N and Canfield P C 2008 *Phys. Rev. Lett.* **101** 057006
- [7] Harmon B N, McQueeney R J, Canfield P C and Goldman A I 2008 *Phys. Rev. B* **78** 184517
- [8] Park T, Park E, Lee H, Klimczuk T, Bauer E D, Ronning F and Thompson J D 2008 *J. Phys.: Condens. Matter* **20** 322204
- [9] Saha S R, Butch N P, Drye T, Magill J, Ziemak S, Kirshenbaum K, Zavalij P Y, Lynn J M and Paglione J 2012 *Phys. Rev. B* **85** 024525
- [10] Lü B, Deng L Z, Gooch M, Wei F Y, Sun Y Y, Meen J K, Xue Y Y, Lorenz B and Chu C W 2011 *Proc. Natl. Acad. Sci.* **108** 15705
- [11] Mittal R, Mishra S K, Chaplot S L, Ovsyannikov S V, Greenberg E, Trots D M, Dubrovinsky L, Su Y, Brueckel Th, Matsuishi S, Hosono H and Garbarino G 2011 *Phys. Rev. B* **83** 054503
- [12] Uhoya W, Tsoi G, Vohra Y K, McGuire M A, Sefat A S, Sales B C, Mandrus D and Weir S T 2010 *J. Phys.: Condens. Matter* **22** 292202
- [13] Kasahara S, Shibauchi T, Hashimoto K, Nakai Y, Ikeda H, Terashima T and Matsuda Y 2011 *Phys. Rev. B* **83** 060505
- [14] Yu W, Aczel A A, Williams T J, Bud'ko S L, Ni N, Canfield P C and Luke G M 2009 *Phys. Rev. B* **79** 020511
- [15] Baek S H, Lee H, Brown S E, Curro N J, Bauer E D, Ronning F, Park T and Thompson J D 2009 *Phys. Rev. Lett.* **102** 227601
- [16] Kawasaki S, Tabuchi T, Wang X F, Chen X H and Zheng G Q 2010 *Supercond. Sci. Technol.* **23** 054004
- [17] Harnagea L, Singh S, Friemel G, Leps N, Bombor D, Abdel-Hafiez M B, Wolter A U, Hess C, Klingeler R, Behr G, Wurmehl S and Büchner B 2010 arxiv:1011.2085v1 [cond-mat.supr-con]
- [18] Goldman A I, Kreyssig A, Prokes K, Pratt D K, Argyriou D N, Lynn J W, Nandi S, Kimber S A J, Chen Y, Lee Y B, Samolyuk G, Leão J B, Poulton S J, Bud'ko S L, Ni N, Canfield P C, Harmon B N and McQueeney R J 2009 *Phys. Rev. B* **79** 024513
- [19] Pratt D K, Zhao Y, Kimber S A J, Hiess A, Argyriou D N, Broholm C, Kreyssig A, Nandi S, Bud'ko S L, Ni N, Canfield P C, McQueeney R J and Goldman A I 2009 *Phys. Rev. B* **79** 060510
- [20] Ji W, Yan X W and Lu Z Y 2011 *Phys. Rev. B* **83** 132504
- [21] Yildirim T 2009 *Phys. Rev. Lett.* **102** 037003
- [22] Zhang Y Z, Kandpal H C, Opahle I, Jeschke H O and Valenti R 2009 *Phys. Rev. B* **80** 094530
- [23] Saha S R, Butch N P, Kirshenbaum K, Paglione J and Zavalij P Y 2009 *Phys. Rev. Lett.* **103** 037005
- [24] Baek S H, Curro N J, Klimczuk T, Bauer E D, Ronning F and Thompson J D 2009 *Phys. Rev. B* **79** 052504
- [25] Moriya T and Ueda K 1974 *Solid State Commun.* **15** 169
- [26] Kimber S A J, Argyriou D N, Yokaichiya F, Habicht K, Gerischer S, Hansen T, Chatterji T, Klingeler R, Hess C, Behr G, Kondrat A and Büchner B 2008 *Phys. Rev. B* **78** 140503
- [27] Zhao J, Huang Q, de la Cruz Clarina, Lynn J W, Lumsden M D, Ren Z A, Yang J, Shen X L, Dong X L, Zhao Z X and Dai P C 2008 *Phys. Rev. B* **78** 132504
- [28] Yamashita H, Yashima M, Mukuda H and Kitaoka Y 2010 *Physica C* **470** 375
- [29] Ueda K 1976 *Solid State Commun.* **19** 965
- [30] Xiao H, Hu T, Dioguardi A P, apRoberts-Warren N, Shockley A C, Crocker J, Nisson D M, Viskadourakis Z, Tee Xianyang, Radulov I, Almasan C C, Curro N J and Panagopoulos C 2012 *Phys. Rev. B* **85** 024530